

Field Measurement and Finite-Element Modeling of Circular and Rectangular Shaft Shapes in the Coeur d'Alene Mining District, Idaho

By Michael J. Beus and Samuel S. M. Chan



UNITED STATES DEPARTMENT OF THE INTERIOR



Report of Investigations 8972

Field Measurement and Finite-Element Modeling of Circular and Rectangular Shaft Shapes in the Coeur d'Alene Mining District, Idaho

By Michael J. Beus and Samuel S. M. Chan



UNITED STATES DEPARTMENT OF THE INTERIOR
Donald Paul Hodel, Secretary

BUREAU OF MINES
Robert C. Horton, Director

Library of Congress Cataloging in Publication Data:

Beus, Michael J

Field measurement and finite-element modeling of circular and rectangular shaft shapes in the Coeur d'Alene mining district, Idaho.

(Report of investigations / United States Department of the Interior, Bureau of Mines ; 8972)

Bibliography: p. 18-19.

Supt. of Docs. no.: I 28.23:8972.

1. Mine shafts--Mathematical models. 2. Rock deformation--Coeur d'Alene Mountains (Idaho and Mont.). 3. Ground control (Mining). 4. Finite element method. 5. Mines and mineral resources--Coeur d'Alene Mountains (Idaho and Mont.). I. Chan, Samuel S. M. II. Title. III. Series: Report of investigations (United States. Bureau of Mines) ; 8972.

TN23.U43 [TN283] 622s [622'.25] 85-600055

CONTENTS

	<u>Page</u>
Abstract.....	1
Introduction.....	2
Acknowledgments.....	2
Description of the test site.....	2
In situ stress and physical properties.....	3
Initial shaft construction.....	4
Instrumentation.....	5
Instrument installation and circular shaft deepening.....	6
Rectangular shaft deepening.....	10
Data analysis.....	13
Finite-element modeling.....	15
Conclusions.....	17
References.....	18
Appendix.--Blasting history, displacement traces, and displacement records.....	20

ILLUSTRATIONS

1. Location of Caladay project in Coeur d'Alene mining district.....	3
2. Plan view of test site at Caladay project.....	3
3. Schematic of station and test shafts.....	5
4. Components of TSR measurement system.....	6
5. Plan view of test shafts showing locations of TSR gauges.....	6
6. Data acquisition equipment installed in instrumentation room.....	7
7. Circular test shaft with blast protection boxes in place over TSR gauges.	8
8. Completed circular shaft partially backfilled to allow access to measure- ment depth.....	9
9. Preparation for initial blast round in rectangular shaft.....	10
10. TSR gauges installed in end wall of rectangular shaft.....	11
11. Completed rectangular test shaft showing location of TSR gauges.....	12
12. Deformation around circular test shaft measured with TSR gauges as a function of shaft advance.....	13
13. Deformation around rectangular test shaft measured with TSR gauges as a function of shaft advance.....	13
14. Relative orientation of shafts with stress field and instrument locations	15
15. Two-dimensional finite-element mesh simulating 8-ft-diam circular shaft..	15
16. Two-dimensional finite-element mesh simulating 5- by 10-ft rectangular shaft.....	16
17. Relative displacement versus distance from circular shaft walls.....	17
18. Relative displacement versus distance from rectangular shaft walls.....	17
A-1. Displacement trace for TSR4 around circular shaft.....	21
A-2. Displacement trace for TSR5 around circular shaft.....	21
A-3. Displacement trace for TSR6 around circular shaft.....	22
A-4. Displacement trace for TSR4 around rectangular shaft.....	22
A-5. Displacement trace for TSR5 around rectangular shaft.....	23
A-6. Displacement trace for TSR8 around rectangular shaft.....	23

TABLES

1. In situ stress, Caladay project.....	4
2. Physical properties, Caladay project.....	4
3. Measured and theoretical displacement.....	17

TABLES--Continued

	<u>Page</u>
A-1. Blasting history of circular and rectangular test shafts.....	20
A-2. Circular test shaft, displacement record.....	20
A-3. Rectangular test shaft, displacement record.....	20

UNIT OF MEASURE ABBREVIATIONS USED IN THIS REPORT

ft	foot	pct	percent
in	inch	psi	pound per square inch
pcf	pound per cubic foot	s	second

FIELD MEASUREMENT AND FINITE-ELEMENT MODELING
OF CIRCULAR AND RECTANGULAR SHAFT SHAPES
IN THE COEUR d'ALENE MINING DISTRICT, IDAHO

By Michael J. Beus¹ and Samuel S. M. Chan²

ABSTRACT

This Bureau of Mines report describes a field experiment involving the sinking of two test shafts to directly compare the deformational behavior of circular and rectangular shapes. Results show that the circular shape is less sensitive to geologic discontinuities and applied stress field. Also, the rectangular shape is subject to a variety of behavioral modes, including beam bending and buckling. Geologic discontinuities around circular and rectangular shapes influence displacement significantly. Simple, two-dimensional elastic finite-element modeling, simulating circular and rectangular shapes in a biaxial stress field, shows that the structural response of a shaft is largely controlled by geologic structure. Consideration of anisotropy may be required for realistic analysis of a deep shaft.

¹Mining engineer, Spokane Research Center, Bureau of Mines, Spokane, WA.

²Mining engineer, Spokane Research Center, Bureau of Mines, Spokane, WA; professor of mining engineering, University of Idaho, Moscow, ID.

INTRODUCTION

Structural design data for shafts and support systems for deep mines are scarce, and research is needed to establish shaft and support design criteria (11).³ Such data would be useful to the mining industry during shaft sinking operations to access deep-seated ore bodies.

Today, many older mining districts, such as the Coeur d'Alene in northern Idaho, experience a dilemma. Circular, concrete-lined shafts are known to enhance production and provide superior ground control if surrounding ground stress is uniform. In the Coeur d'Alene district, rectangular, timber-supported shafts have proven adequate over the years and are cheaper to construct, but require excessive maintenance and repair. Annual repair costs may average more than \$100 per foot of shaft according to recent data obtained from deep-mine operators.

In 1972, the Bureau initiated projects to advance the state-of-the-art of shaft

design, particularly in deep, vein-type metal mines. The Coeur d'Alene mining district in northern Idaho, a typical deep-vein mining area, was chosen as the research location because of test site availability and because shaft stability problems were common. The objective of the research was to advance deep-shaft design technology using rock mechanics and structural analysis techniques.

This report presents the results of part of this research, compares measured deformational behavior of circular and rectangular shaft shapes, and compares these measurements with simple finite-element analyses. The project involved construction and monitoring of two test shaft openings, one with a circular cross section and the other with a rectangular cross section. The resulting field data form the basis for a comparative evaluation of these two common shaft shapes.

ACKNOWLEDGMENTS

Mining companies and personnel in the Coeur d'Alene mining district provided technical assistance and test sites for the fieldwork. Particularly helpful were James Robison, project

superintendent, Callahan Mining Corp., and Lovon Fausett, president, Wallace Diamond Drill Co. Their support is gratefully acknowledged.

DESCRIPTION OF THE TEST SITE

The Coeur d'Alene mining district is situated in the Coeur d'Alene Mountains of Shoshone County, ID. The main rock in the district is the Precambrian metamorphics of the Belt Supergroup with a maximum thickness of 28,000 ft (9). Mineralization occurs mainly in the St. Regis and Revett Formations in the middle of the Belt rocks. The St. Regis is geologically younger than the Revett Formation. Both consist mainly of interbedded, fine-grained quartzite and argillite and dip steeply with numerous overturned beds.

The main structural feature in the district is the Osburn Fault, which strikes west-northwest and has extensive displacement.

Most major mines in the district are located near the Osburn Fault or its branches. The mineral deposits occur as steeply dipping, quartzsiderite veins containing silver-bearing tetrahedrite, galena, and sphalerite. The main mining method is horizontal cut-and-fill stoping with conventional drill, blast, and mucking cycles. Hoist and rail haulage are primary means for transporting ore, rock, and materials. Rock bolting, timbering, and hydraulic sandfilling are used for ground support. Shafts in the

³Underlined numbers in parentheses refer to items in the list of references preceding the appendix.

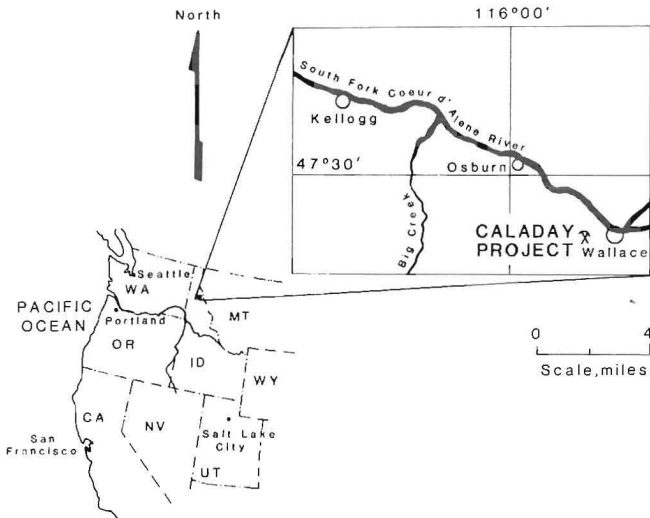


FIGURE 1. - Location of Caladay project in Coeur d'Alene mining district.

district extend to more than 3,000 ft below sea level and more than 8,000 ft below the ground surface.

The Caladay project is located on the south side of the Osburn Fault, 1 mile west of Wallace, ID (fig. 1). Existing development at the time the site was made available included a main adit, several short crosscuts, a shaft station, and related excavations. The test shafts were constructed at the existing shaft station 5,200 ft inside the portal of the main adit under about 1,200 ft of overburden. This depth was considered adequate to simulate geologic conditions that may be encountered at greater depths, owing to the steep dip of the structure and the vertical continuity of rock types. The

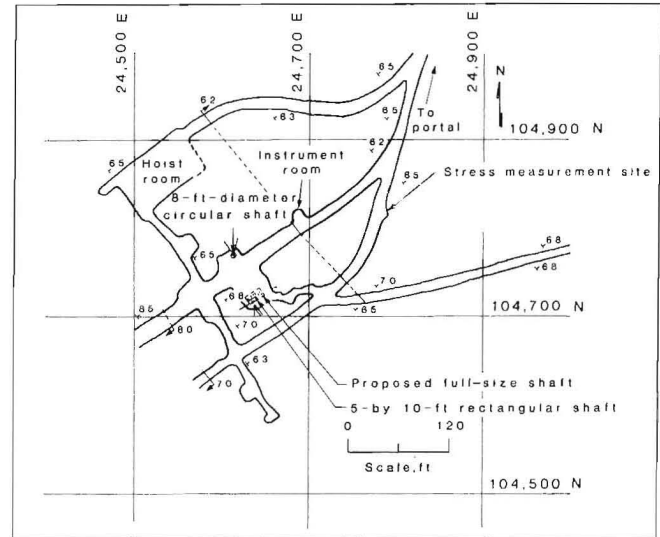


FIGURE 2. - Plan view of test site at Caladay project.

relative effect of the absolute stress magnitude may also be extrapolated to greater depth if desired.

Figure 2 shows the complete excavation layout, the proposed test shafts, the hoist room, and the connecting drifts. The country rock in the area consists of steeply dipping, argillaceous St. Regis quartzite of Precambrian age with numerous gouge-filled joints, partings, and minor faults. Strata in the area strike roughly northwest at 35° to 45° and dip 65° to 70° to the northeast. The site lies about 300 ft above the adjacent valley floor. There is no excavation between the test shaft area and the ground surface except the initial station excavation and the rope raise.

IN SITU STRESS AND PHYSICAL PROPERTIES

To properly assess the in situ conditions and to provide input for mathematical modeling, the stress field and material properties at the test site were determined.

CSIR (Council for Scientific and Industrial Research) biaxial strain cells were used to measure in situ stress. The basic principles of the biaxial strain cell technique have been well documented (13-14), and details of the application of this technique in the Coeur d'Alene

mining district have been described previously (3, 6). The results of the in situ stress and physical property measurements of rocks from the Caladay site are listed in tables 1 and 2.

The major, intermediate, and minor principal stresses at a depth of 1,200 ft are calculated as 1,854 psi at $S 80^\circ E$ plunging $54^\circ W$, 960 psi at $S 44^\circ W$ plunging $20^\circ SW$, and 696 psi at $N 31^\circ W$ plunging $29^\circ W$, respectively. The measured vertical stress was 1,450 psi and was

TABLE 1. - In situ stress, Caladay project

In situ stress	psi	Bearing	Plunge	In situ stress	psi	Bearing	Plunge
Principal:				Horizontal:			
0-1.....	1,854	S 80° E	54° W	σ_{H_1}	1,280	N 87° E	NAp
0-2.....	960	S 44° W	20° SW	σ_{H_2}	820	S 3° E	NAp
0-3.....	696	N 31° W	29° NW	Vertical: σ_v	1,450	NAp	NAp

NAp Not applicable.

TABLE 2. - Physical properties, Caladay project

Modulus of elasticity (E).....	psi..	9.58 × 10 ⁶
Internal friction angle (ϕ).....	deg..	50.5
Uniaxial compressive strength, psi:		
σ_{0°		19,000
σ_{45°		13,000
σ_{90°		23,000
Triaxial compressive strength, psi:		
σ_{500}		24,000
σ_{1000}		29,000
σ_{1500}		34,000
σ_{3000}		42,000
σ_{6000}		49,000
Poisson's ratio (ν).....		0.21
Cohesion (c).....	psi..	2,980
Tensile strength (σ_τ), psi:		
Direct.....		1,600
Indirect.....		2,220

found to be similar to the theoretical stress value calculated from a gravity load using a unit weight of overburden rock of 165 pcf. Maximum and minimum horizontal stress values are 1,280 psi at N 87° E and 820 psi at S 3° E, respectively.

Preliminary field testing at the Caladay also included in situ measurement of the modulus of deformation using the Colorado School of Mines (CSM) dilatometer (10). The average in situ modulus of deformation of the Caladay rock ranges from 2.6 × 10⁶ psi to 9.6 × 10⁶ psi, depending on orientation of the bedding planes (16). Laboratory values for modulus of elasticity average 9.6 × 10⁶ psi, and Poisson's ratio averages

0.21. Values for the internal friction angle, cohesion, and compressive and tensile strength are also shown in table 2. The statistical variance, although not listed, ranges from 31 pct for direct tensile strength to 6 pct for unconfined compressive strength. The compressive strength increases significantly with increased confining pressure. Although rock strength varies widely, most rocks exhibited linear deformation and behaved elastically under both uniaxial and triaxial loads. Most of the competent rock samples burst violently at failure during laboratory strength tests, indicating their brittle nature and their capacity for storage of elastic strain energy.

INITIAL SHAFT CONSTRUCTION

Shaft construction was initiated after a cooperative agreement was negotiated and signed between the Bureau and Callahan Mining Co. Wallace Diamond Drill Co., a local mining contractor,

constructed the shafts, and Callahan provided compressed air, water, electricity, and transportation of personnel and materials.

The plan called for sinking an 8-ft-diam circular shaft to a depth of 27 ft in the tail-room area of the existing shaft station. This was to be followed by a 5- by 10-ft rectangular shaft of similar depth within the boundaries of a proposed full-size shaft. The shafts were oriented with the long axis normal to the strike of the bedding, in accordance with standard practice in the district. Figure 3 is a schematic of the proposed test shafts located in the existing shaft station with the instrument locations indicated.

The contractor's equipment included an air-track mobile drifter drill, sinker drills, a 3/4-ton backhoe, an air-motor-powered clam bucket for mucking, and a small front-end loader. The excavation sequence for both shafts required first drilling and blasting a small round to create a 1-1/2-ft lip around the opening. This would protect the installed instruments from later blast damage and would remove any surface material damaged by previous blasting. After installation of the instruments, it was intended that six successive 4-ft drill and blast rounds would advance the shaft bottom to the required depth. Smooth wall blasting techniques were used to presplit the periphery of the excavation. This

decreased overbreak, which would endanger the measuring points, and lessened damage to the adjacent wall rock.

To minimize the effects of time between successive rounds and to decrease interference with instrumentation, the shafts were predrilled to final depth. The holes were then completely filled with iron oxide sand. The sand was removed in approximately 4-ft intervals to accommodate the blasting agent to the required depth. The remainder of each hole in the shaft bottom was thus protected from blast damage from the preceding round.

INSTRUMENTATION

The instrumentation used in this study was developed and patented by the Bureau in 1971 (19). It is called a tunnel stress relaxation (TSR) gauge and is designed to measure radial deformation around underground openings during excavation.

The TSR system consists of a probe (extension tube and transducer head), a deformation-sensing anchor, an adjustable mounting head, and an anchored support reference pipe (fig. 4). The sensing anchor epoxied into the end of a borehole drilled adjacent to the proposed opening. The ball on the end of the transducer

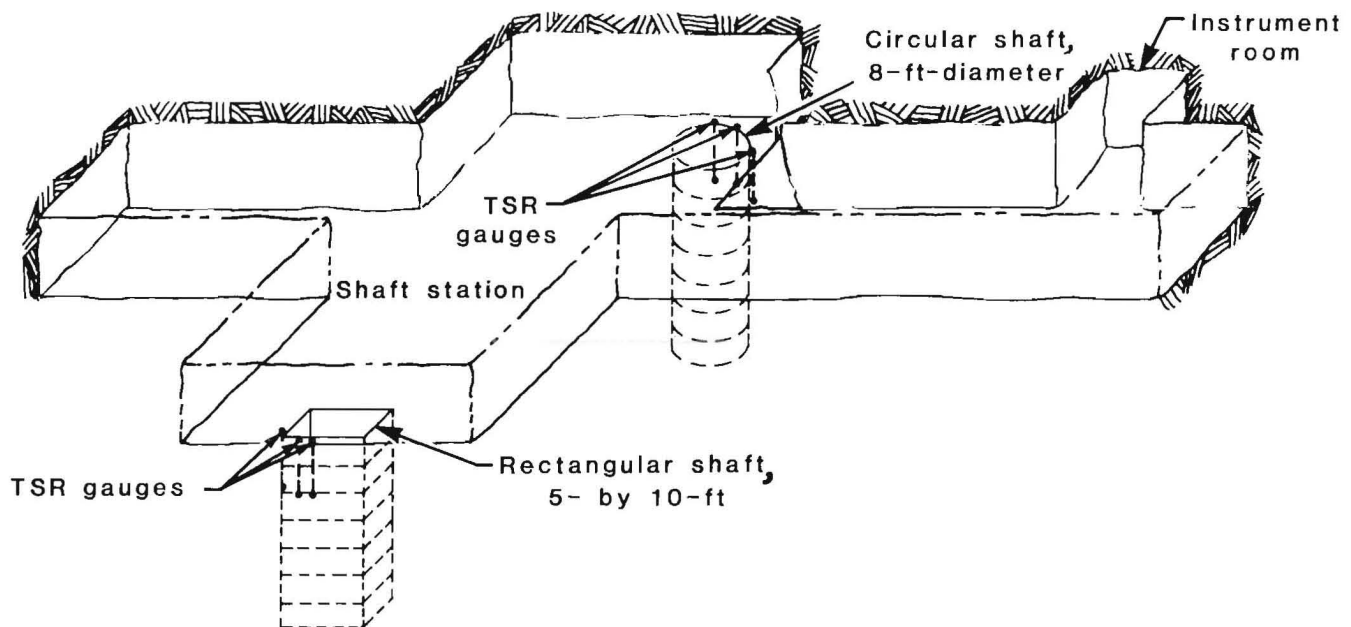


FIGURE 3. - Schematic of station and test shafts.

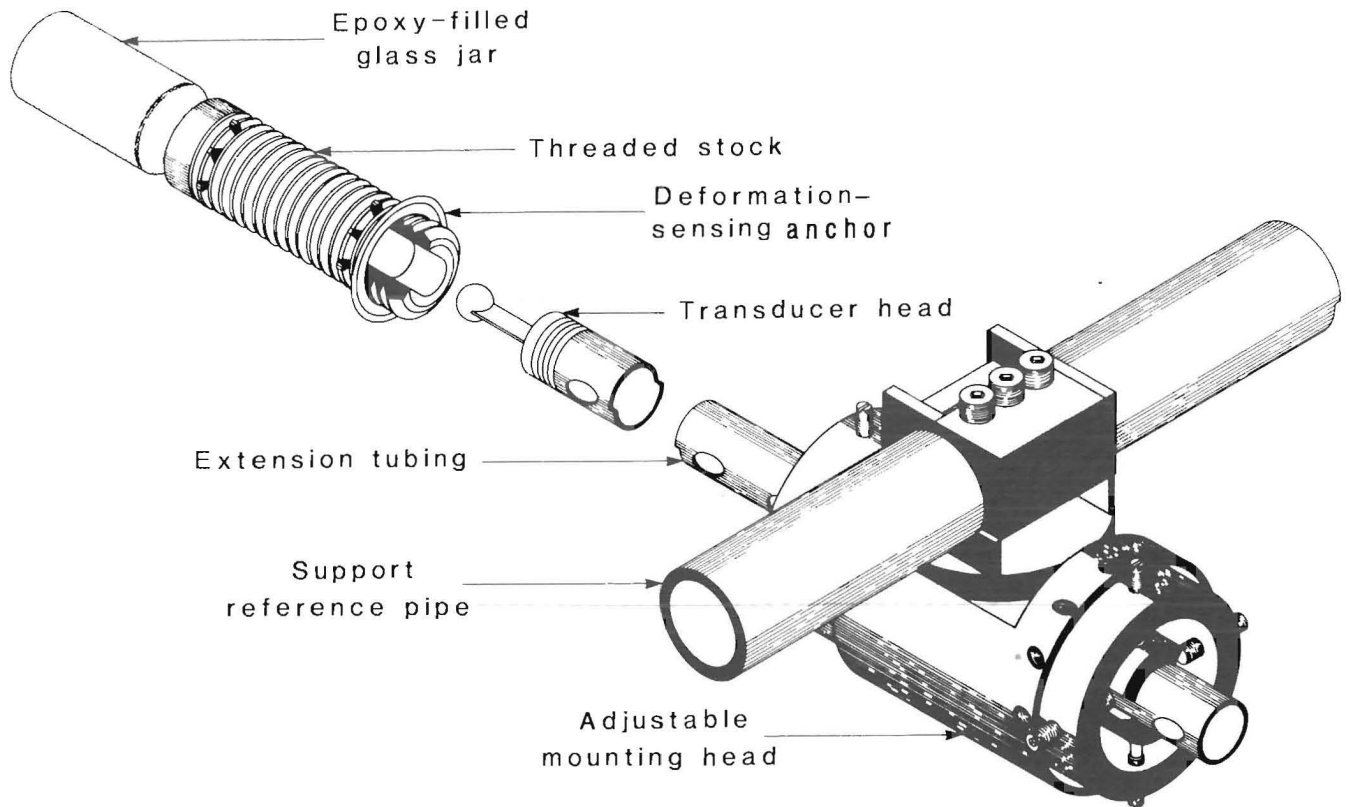


FIGURE 4. - Components of TSR measurement system.

head is then inserted into the socket end of the anchor. Movement of the anchor resulting from excavation causes deflection of the probe. The probe is rigidly clamped to a support reference pipe by an adjustable mounting head. The support pipe is grouted into the wall rock as the transducer reference. The mounting head permits three-dimensional adjustment of the probe for proper preload, orientation, and depth. Detailed descriptions of the design and testing of the TSR system have been published (5, 18).

INSTRUMENT INSTALLATION AND CIRCULAR SHAFT DEEPENING

After excavation of the initial 1-1/2 ft for the circular shaft, holes for the TSR gauge installation were drilled. A concrete pad was poured at each instrument location for proper collaring of the instrument installation hole. Three vertical 3-in-diam holes were drilled to a depth of about 7 ft. Figure 5 shows

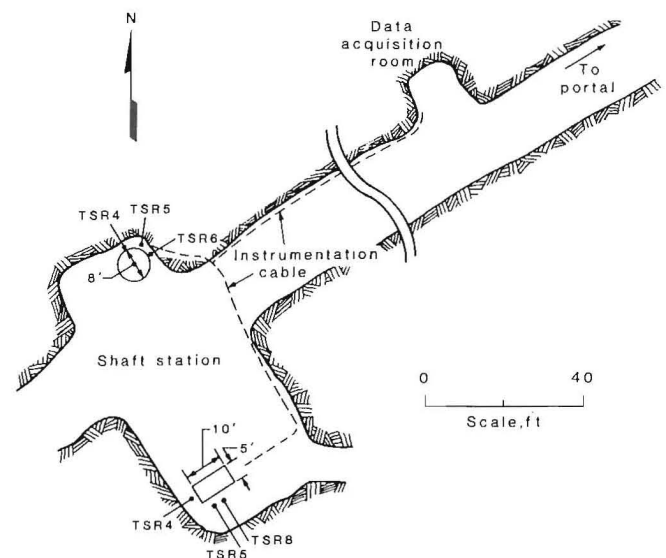


FIGURE 5. - Plan view of test shafts showing locations of TSR gauges.

the instrumentation plan for both shafts. The holes were angled about 2° , with the downhole anchor located about 12 in from the shaft wall. Instrument holes were

positioned around the circular shaft perimeter at 0°, 45°, and 90°. This positioning allows measurement of deformation perpendicular, parallel, and at 45° to the bedding, in the horizontal plane. The reference anchor holes were then drilled into the station walls. Heavy-wall pipe was inserted and anchored to a depth of 5 ft with Lumnite⁴ quicksetting alumina cement.

The deformation-sensing anchors were installed around the shaft at the 7-ft depth-sensing plane with POR-ROK expanding cement. The TSR gauges were

⁴Reference to specific products does not imply endorsement by the Bureau of Mines.

installed and secured into the adjustable mounting heads. Heavy-gauge steel boxes were placed over the TSR gauges and rock-bolted to the concrete drilling pad for blast protection. The electrical lead wires were routed up through the boxes in flexible conduit into 3-in-diam holes drilled into the nearby shaft pillar and terminated at the data acquisition room.

The predrilled holes were blown free of sand to a depth of 3 to 4 ft and loaded with Gelex dynamite. The installation was covered with sand to prevent fly-rock and minimize vibration of the instrumentation.

Data acquisition was conducted about 200 ft from the shaft area (fig. 6), using conventional data acquisition

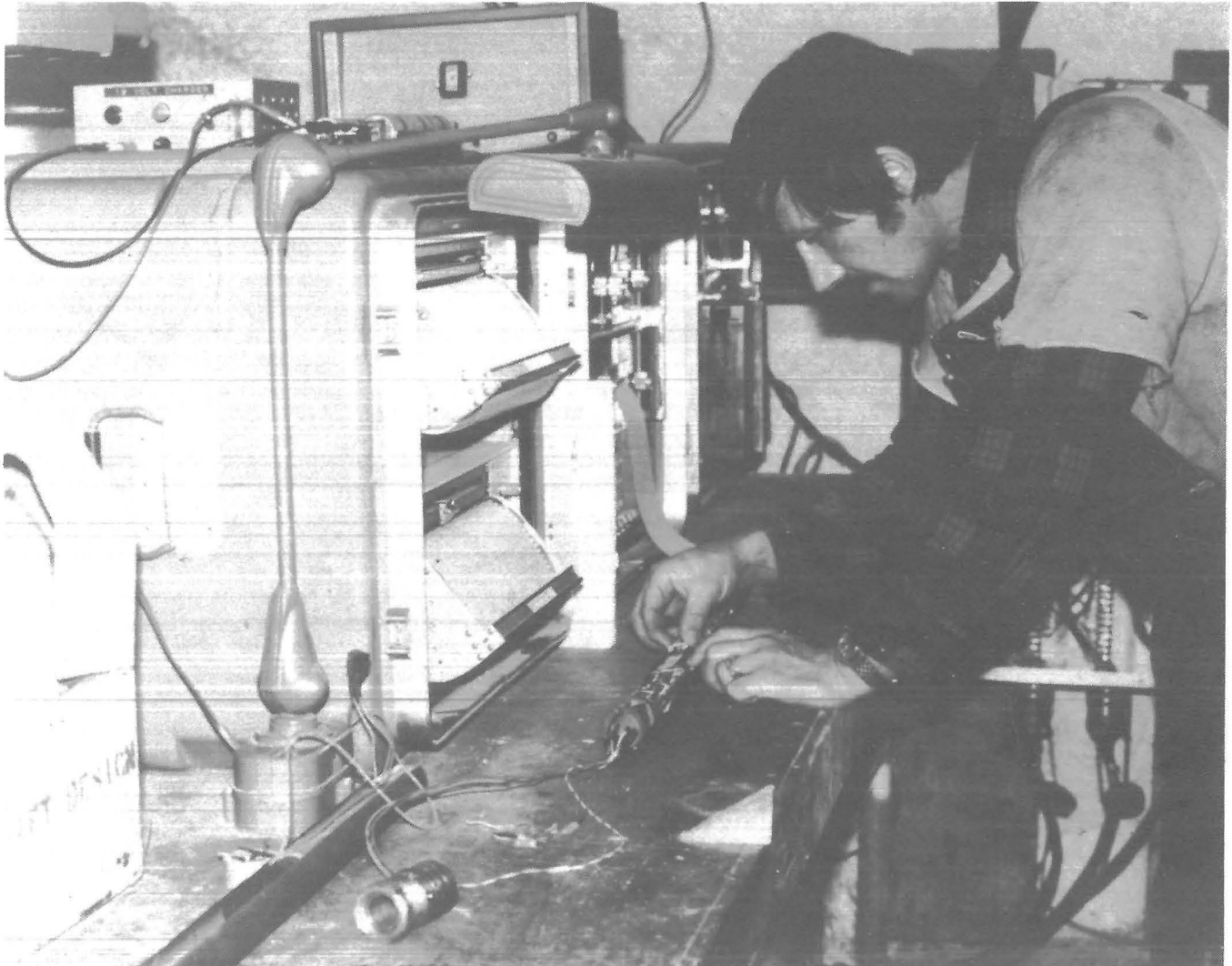


FIGURE 6. - Data acquisition equipment installed in instrumentation room.

equipment modified for underground application (15). The data acquisition room included strip chart recorders to give a visual indication of rock movement sensed by each TSR gauge during blasting and conventional strain indicators for backup to the automatic system. Blasting was controlled from the data acquisition room, and excavation was coordinated with the scan time to maximize data output.

After the TSR gauges were installed, excavation commenced with time intervals between rounds for the rock to stabilize. Beyond the 7-ft depth, the sand cushion was eliminated because flyrock was no longer a hazard. The collar of the shaft was stabilized with landing mat secured by rock bolts. To a depth of about 10 ft, shaft muck was removed with a backhoe; below that depth a slusher-clam bucket was used. A train loader transported the muck to the surface dump.

Considerable water was encountered during sinking, and continual pumping was necessary.

Final depth of the circular shaft after eight rounds blasted over a period of about 2 weeks was 24 ft, about 16 ft beyond the TSR sensing plane. Figure 7 shows the TSR gauges installed around the completed circular shaft. Figure 8 shows the TSR sensing depth with the bedding planes clearly visible. Recording continued for several weeks after completion of the sinking operation to register possible time-dependent deformation. Table A-1 (appendix) shows the blasting history for the circular test shaft. The circular shaft was completely backfilled with muck after the instruments were removed and capped with 2 ft of reinforced concrete, to serve as a foundation for a proposed hoist.

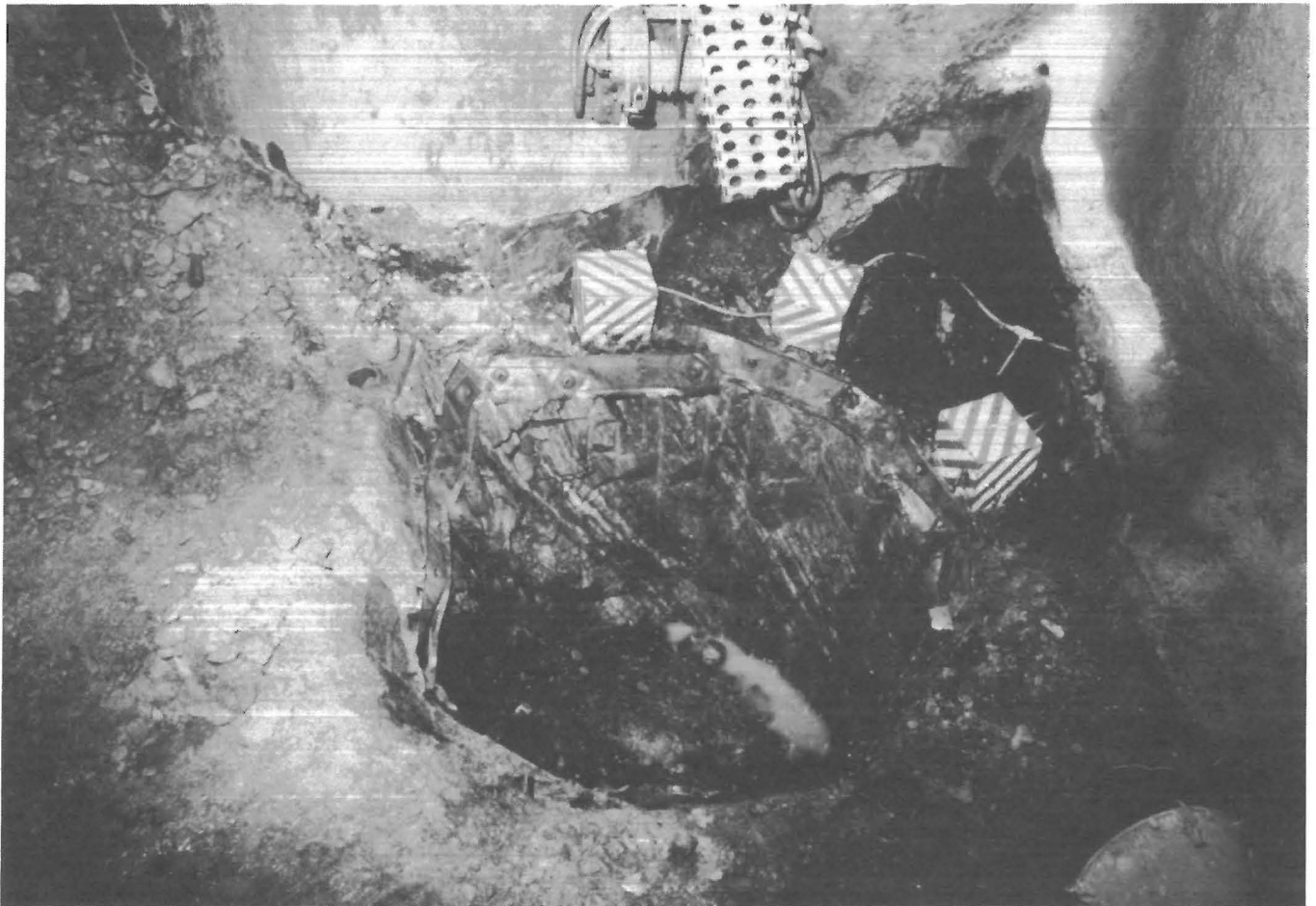


FIGURE 7. - Circular test shaft with blast protection boxes in place over TSR gauges.

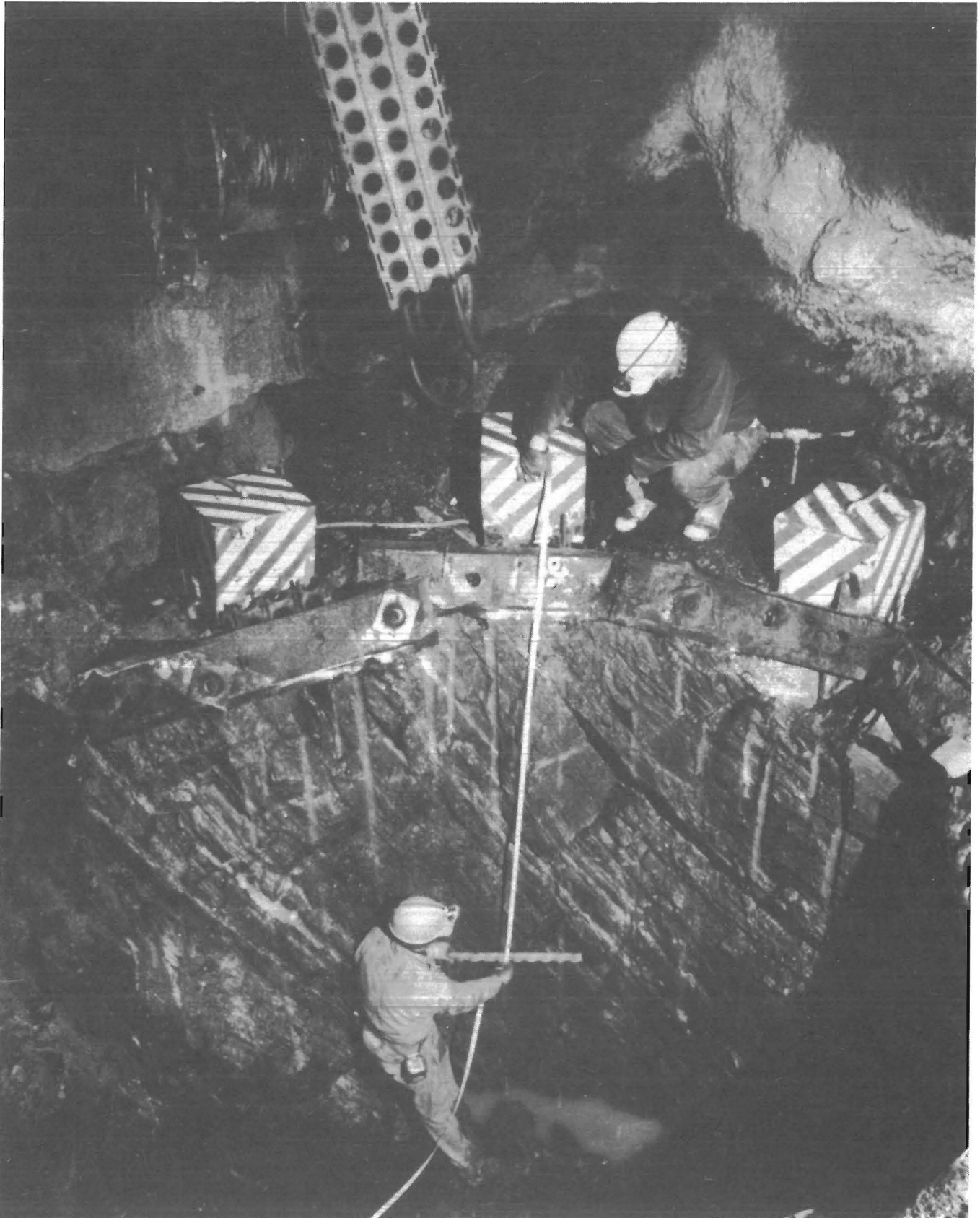


FIGURE 8. - Completed circular shaft partially backfilled to allow access to measurement depth.

RECTANGULAR SHAFT DEEPENING

Instrument installation and excavation procedures used for the rectangular shaft were similar to those used for the circular shaft. Figure 9 shows the initial blast round being wired up, and figure 10 shows a TSR gauge installed in the endwall of the shaft to measure deformation normal to the bedding. The other TSR gauges were installed at the center of the long dimension, and halfway between

the corner and center, to measure deformation parallel to the bedding (figures 5 and 11). The endwall of this shaft was very argillitic, and considerable rock bolting was required to maintain stability. Eventually, the endwall strata sloughed, exposing the sensing anchor. Timber bulkheads were also required around the collar of the shaft to stabilize the badly fractured rock.

A 21-ft-long, fully grouted pipe with 3-ft side braces was needed for the TSR



FIGURE 9. - Preparation for initial blast round in rectangular shaft.



FIGURE 10. - TSR gauges installed in end wall of rectangular shaft.



FIGURE 11. - Completed rectangular test shaft showing location of TSR gauges.

gauge mount because of the distance between the shaft collar and the station walls. The reference anchor pipe was completely encased in 2- by 8-in timber frames and packed with sand to dampen blasting vibrations and to protect against flyrock. The TSR gauge holes were collared 24 in (36 in on TSR4) back from the shaft edge because of poor collar conditions, and the drill hole was angled to put the sensing anchor points within 12 in of the shaft wall.

The rectangular shaft contained forty-three 2-in holes, including the pre-split holes, with a center burn and four 3-in surrounding relievers. The 5- by 10-ft cross section was excavated using 3- to 4-ft full-face blast rounds and by

mucking with the backhoe and clamshell. Before charging, sand was removed from each hole with a blowpipe to the required depth. The rectangular shaft was excavated with seven consecutive rounds to an approximate final depth of 26 ft, roughly 17 ft beyond the TSR sensing plane. Continual pumping was also required in this shaft for water removal.

Table A-1 (appendix) shows the blasting history over a period of 3 weeks. The TSR gauges remained installed around the rectangular shaft for about 5 months to record any long-term deformation. The site was thoroughly cleaned before abandonment, and a safety railing was installed.

DATA ANALYSIS

The deformation records from the TSR gauges corresponding to circular and rectangular shaft advance are shown in figures 12 and 13, respectively, with shaft closure shown as positive. The shaft advance corresponds to the individual blast rounds, each lasting about 13 s. The total measured displacement is

listed in tables A-2 and A-3 (appendix) for the circular and rectangular shapes,

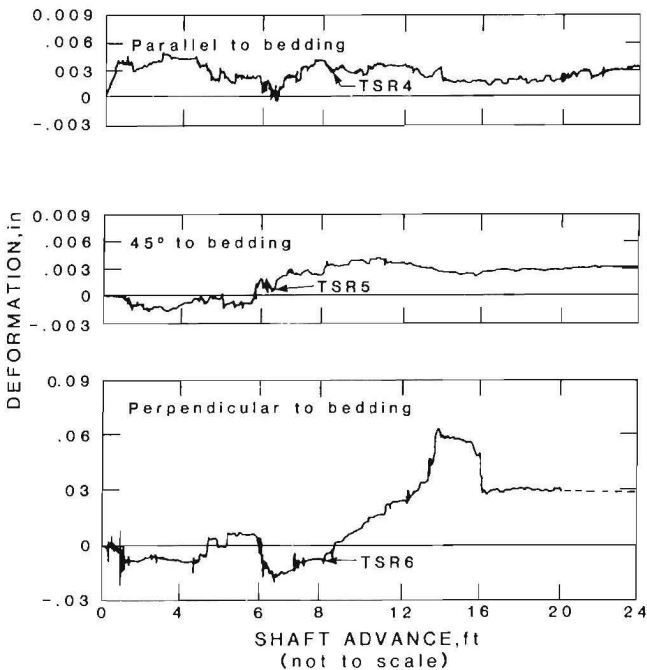


FIGURE 12. - Deformation around circular test shaft measured with TSR gauges as a function of shaft advance.

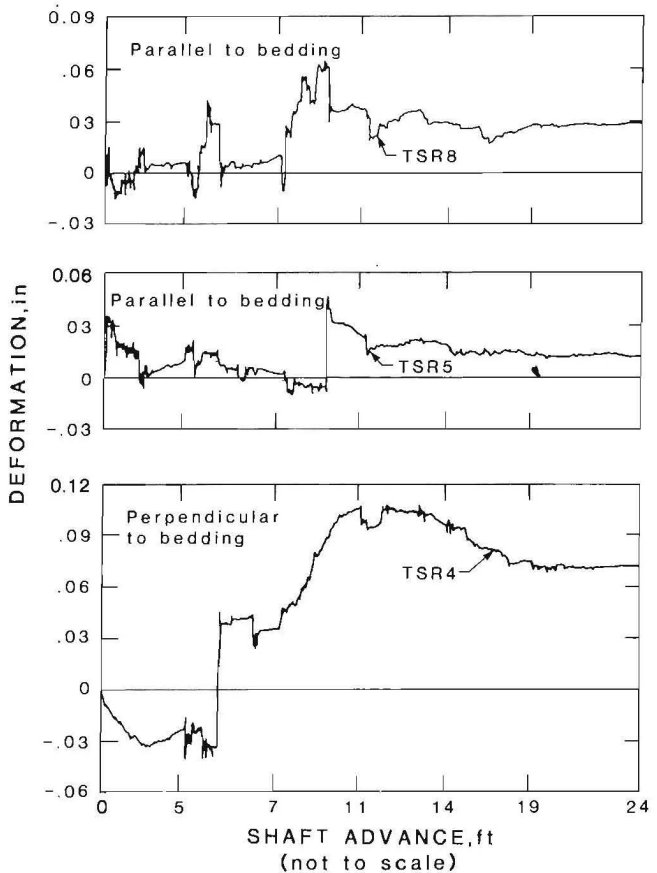


FIGURE 13. - Deformation around rectangular test shaft measured with TSR gauges as a function of shaft advance.

respectively. The actual deformation trace of each instrument is shown in the appendix in figures A-1 through A-6.

The displacement shown in figures 12 and 13 has been adjusted to eliminate extraneous effects of the construction environment (blasting, water, etc.) from actual rock response. Based on previous experience with this type of instrumentation in a similar environment, certain malfunctions were expected, and representative "signatures" in the instrument response pattern could be identified. These response patterns are typical for instruments subject to blasting, water, and mechanical damage from construction activities.

These malfunctions have been classified as either intermittent or progressive. Intermittent malfunctions are characterized by data showing recurring offsets. Progressive malfunction was characterized by a low-level exponential decay from stable trends of the previous readings. Other sources of error include anchor slippage or readjustment due to blasting, and "bedding in" of the anchors. In screening and correcting the data, all instances of exponential decay, recurrent offsets, or single-point anomalies were evaluated individually and adjusted as required.

In figure 12, the displacement parallel to the bedding (TSR4) shows that the rock trended toward a net displacement almost immediately. TSR5, 45° to the bedding, indicates an initial abutment load resulting from blast pressure. As the shaft advanced from 6 to 16 ft, there was a closure trend with a gentle relaxation throughout the remainder of the excavation. Displacement normal to the bedding (TSR6) showed a slight abutment load up to 6-ft depth and then a steady closure excursion from 6 to 16 ft with about one-half of the total closure being recovered beyond 16 ft. The deformation is significantly dampened at 16 ft, and movement is barely discernible after 20 ft. The oscillations during each blast reflect the individual delays in the round. The displacement indicated by TSR6, normal to bedding, is an order of magnitude greater than that indicated by the other

two gauges. This difference is attributed to bedding plane anisotropy and possible rock mass separation.

Figure 13 shows the displacement of the rock around the rectangular shaft. Displacements parallel with the bedding (TSR8 and TSR5) show oscillations about the zero point up to the 7-ft shaft depth. As the shaft advances from 7 to 14 ft, a significant closure trend is evident. The shaft wall displacement shown by TSR8, located midway on the shaft longwall, is about twice that of TSR5, located midway between TSR8 and the corner of the shaft. As the excavation proceeds to 24 ft, displacement oscillations lessen, with the final net closure as indicated.

Displacement normal to the bedding (TSR4) shows a large initial abutment load up to 5 ft and a large and rapid closure excursion from 5 to 11 ft. From 11 to 19 ft, this closure is gradually relaxed, with the final blast producing minimal deformation. The net closure normal to the bedding (TSR4) is more than twice the maximum measured parallel with the bedding (TSR8). This is attributed to individual bedding plane separation and the presence of a thick clay-gouge seam near the TSR4 sensing anchor.

Comparing displacement around the two shaft shapes, the deformation excursions and oscillations are considerably more pronounced around the rectangular shaft than around the circular. Deformation in both shafts was maximum in a direction normal to the bedding planes and minimum parallel with bedding.

The directional properties of the rock structure and bedding are key parameters controlling deformation. The displacement around the rectangular shaft was greater in magnitude at all measured locations than its counterpart around the circular shaft. Relative displacements normal to the bedding for the rectangular and circular shafts were 0.072 in and 0.030 in, respectively, more than a 2:1 ratio. The rectangular shaft was also subjected to the effects of exposure of more weakness planes, all contributing to greater deformation.

FINITE-ELEMENT MODELING

The objective of finite-element analysis is to compare the actual deformation measured in the shaft wall with a simple theoretical model. The computer codes ADINA (2) and BMINES (8, 12) were used to simulate the shafts. The geometry and geologic structure associated with this excavation are relatively complex, and the field data suggest that a three-dimensional, anisotropic analysis is required. However, the scope of the project limited the analysis to two-dimensional, linear elastic, with isotropic, homogeneous material behavior. A three-dimensional elastic model was previously completed and reported on that simulated one-half of the existing shaft station and the complete rectangular test shaft (7).

The physical data used as input were derived from measurements conducted at the test site and in the laboratory

(table 1). These consisted of the field stresses, rock properties, and the geometrical configuration and orientation of the shafts. The major and minor principal stresses are, respectively, 820 psi and 1,280 psi. The major principal stress is aligned along the east-west axis. Figure 14 shows the relative orientation of the shafts with the stress field and instrument locations. Elastic rock properties based on laboratory measurement are--

$$E = 9.58 \times 10^6 \text{ psi (modulus of elasticity),}$$

$$\text{and } \nu = 0.21 \text{ (Poisson's ratio).}$$

The finite-element meshes for the two-dimensional analysis of the circular and rectangular shafts are shown in figures 15 and 16, respectively. Nodal points for these meshes were placed coincident with instrument locations to simplify data reduction. The outside dimension of the mesh was six times the largest dimension of the opening. This provides accuracies within 5 pct of the mesh resolution is fine enough.

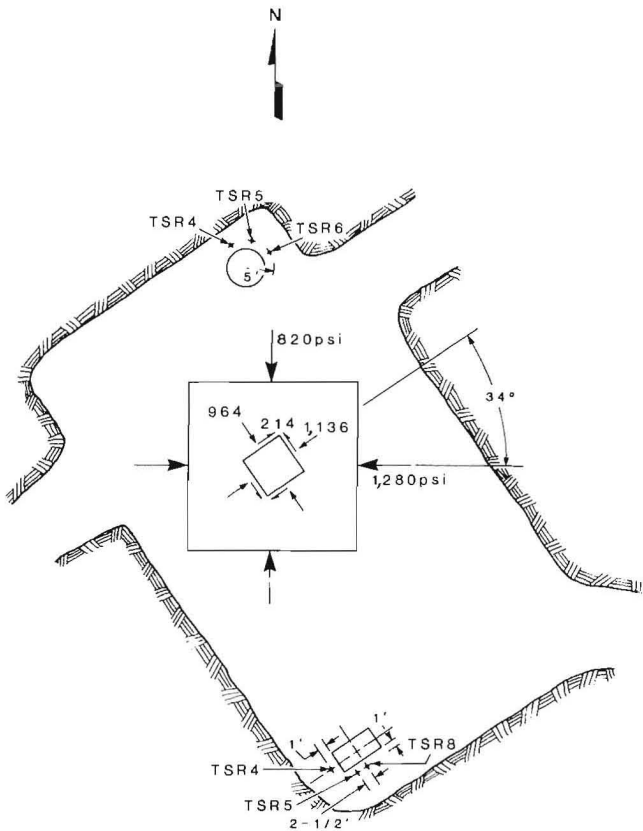


FIGURE 14. - Relative orientation of shafts with stress field and instrument locations.

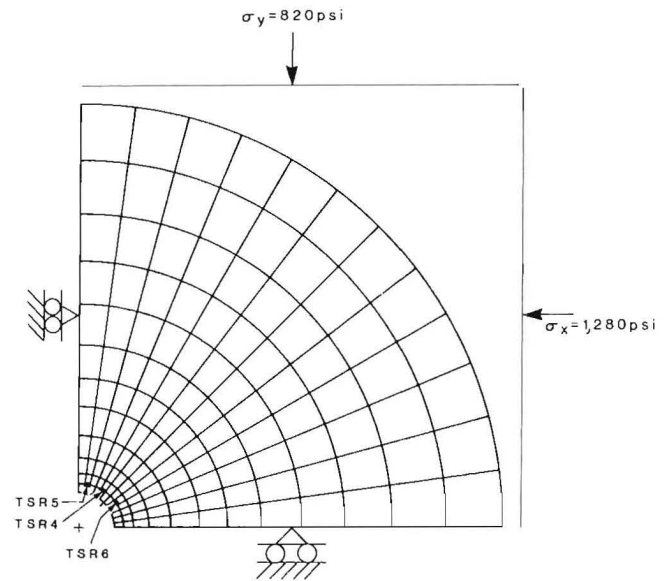


FIGURE 15. - Two-dimensional finite-element mesh simulating 8-ft-diam circular shaft.

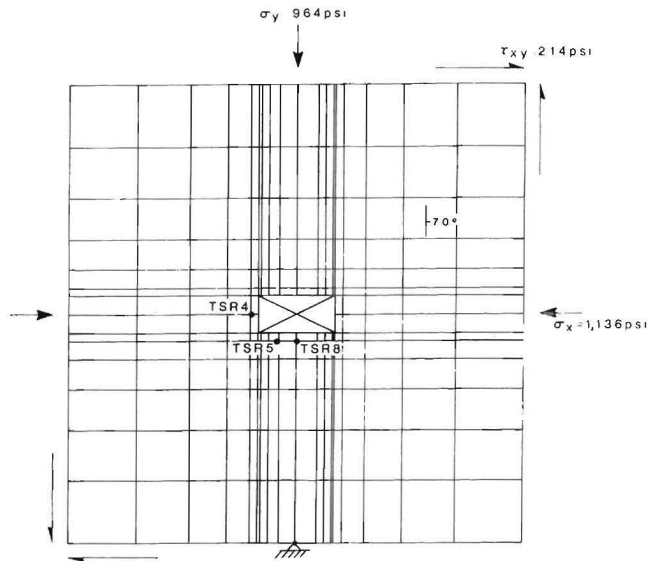


FIGURE 16. - Two-dimensional finite-element mesh simulating 5-by 10-ft rectangular shaft.

Due to symmetry about both axes, with respect to geometry and loading, only the first quadrant of the circular mesh is needed. Instrument locations are shown superimposed on the mesh. The angles to the instrument locations from the horizontal axis are 37° , 52° , and 82° , respectively, which correspond to the actual locations for TSR6, TSR4, and TSR5 with respect to the stress field.

For the rectangular shaft a complete two-dimensional mesh was required owing to asymmetry from the shear stress component. When field stresses are resolved coincident with the principal geometrical axes of the rectangular shape, as shown in figure 16, the magnitude of these resolved stresses is--

Minimum horizontal stress = 964 psi,

Maximum horizontal stress = 1,136 psi,

Shear stress = 214 psi.

The boundary conditions imposed on the rectangular mesh are also shown in figure 16. The bottommost center node is held fixed in both x and y directions. Instrument locations are again indicated for TSR4, TSR5, and TSR8.

The solutions consider an opening in a two-dimensional plate, under plane strain

conditions, subjected to biaxial field stresses. Two solution steps are necessary. In the first step, a solution is found for the uniformly loaded continuous plate. Then, in the second case, the material of the opening is removed, and the analysis is repeated. The desired results are obtained from the linear combination of deformations from these solutions.

Relative displacements are plotted as a function of distance from the shaft walls in figures 17 and 18 for the circular and rectangular shafts, respectively. In both of these plots, the distances from the shaft wall to the instrument sensor location and the instrument reference depth are indicated. The difference in displacement between these two locations is the net radial displacement for the corresponding instrument, which can then be compared to that measured in the field.

The displacement curves all show the same trend. The rate of displacement is greater near the shaft wall and lessens monotonically with increased distance, converging to near zero at the model boundary. Figure 17 indicates a net radial displacement at the TSR4, TSR5, and TSR6 instrument positions of 0.003 in, 0.002 in, and 0.004 in, respectively. This is about 50 pct of the actual measured value at TSR4 and TSR5, and almost an order of magnitude less than that measured at TSR6.

The results of the two-dimensional elastic model simulating the rectangular test shaft are shown in figure 18. The plot indicates a net displacement of 0.008 in, 0.006 in, and 0.004 in for TSR8, TSR5, and TSR4, respectively. This is about 30 pct and 40 pct of that measured at TSR8 and TSR5, and almost two orders of magnitude less than that measured at TSR4. Table 3 lists and compares the results from figures 12, 13, 17, and 18. The theoretical deformation of the rectangular shaft also exceeds the corresponding displacements around the circular shaft at all locations.

Neither of these models compares particularly well with the field results. It is concluded that most of the

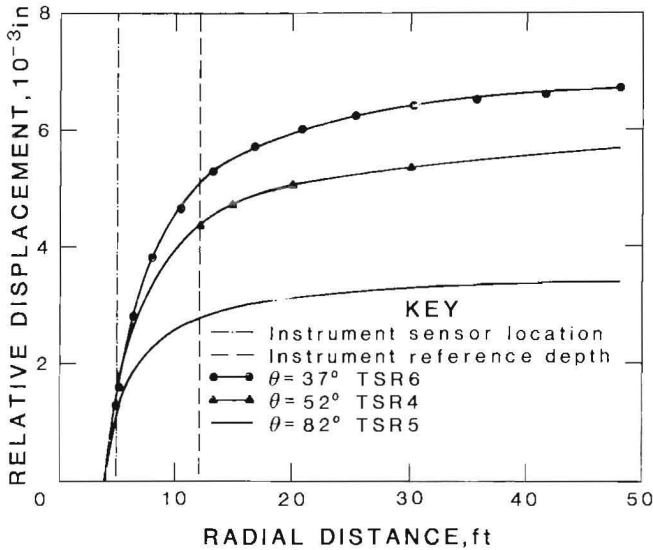


FIGURE 17. - Relative displacement versus distance from circular shaft walls.

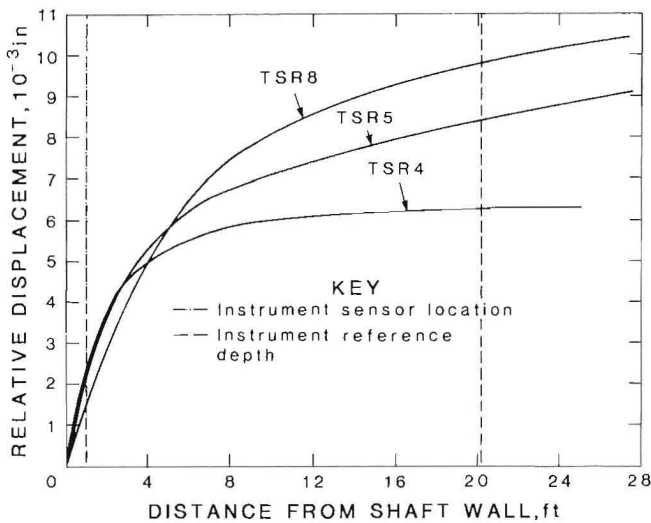


FIGURE 18. - Relative displacement versus distance from rectangular shaft walls.

displacement results from anisotropy and elastic instability of the rock mass and is not a pure elastic response to the applied stress field. A large three-dimensional model which incorporates the anisotropic nature of the rock mass and the complex joint system would more

TABLE 3. - Measured and theoretical displacement

Shaft	Measured	Two-dimensional elastic
Circular:		
TSR4.....	0.005	0.003
TSR5.....	.004	.002
TSR6.....	.030	.004
Rectangular:		
TSR8.....	.030	.008
TSR5.....	.014	.006
TSR4.....	.072	.004

appropriately simulate this behavior. "Attenuation factors" have also been developed (17) to approximate three-dimensional configurations with a two-dimensional model. Another approach currently being pursued is to systematically reduce the modulus and incorporate the effects of anisotropy with a modulus contrast. Recent investigations of anisotropy in the Coeur d'Alene region, based on the "Q" rating system (1), suggest that a 4:1 ratio may exist between modulus values parallel and normal to the bedding.

If this "modulus contrast" and "modulus reduction factor" were to be applied to the Caladay data, the correlation with field data could be much improved, particularly normal to bedding. A cursory analysis shows that the theoretical displacement at the midpoint on the short-wall of the rectangular shaft may be improved to better than one-fourth of the measured value. An even better correlation may be possible for the circular shaft to about 80 pct of the measured value normal to the bedding (TSR6). A more rigorous investigation of all of these factors would require a more detailed analysis and is beyond the scope of this report. As a minimum, consideration of the anisotropic nature of the medium is suggested for any future detailed structural analysis.

CONCLUSIONS

The test shaft openings discussed in this report are intended to simulate construction of full-size shafts and to

measure response of the rock mass to in situ field stress, excavation, and anisotropy. The measured displacement in

both the circular and rectangular shafts agrees well with the projected in situ stress and geologic conditions.

The displacement traces obtained during excavation were characterized by an initial abutment load, indicated by dilation of the shaft walls. The closure excursion that followed, as the face advanced past the measuring points, was much more pronounced around the rectangular opening. Displacements generally ceased as a shaft face approached a depth twice the diameter of the excavation (about 17 ft) beyond the TSR sensing plane.

The smallest displacements were measured at the 0° and 45° positions of the circular shaft (parallel and 45° to the bedding), and between the center and the corner of the long axis of the rectangular shaft. Maximum displacement occurred normal to the bedding for both the circular and the rectangular shaft and was extreme to the point of failure in the end wall of the rectangular shaft. The smaller and more uniform displacement around the circular shaft is considered a result of the confining effect of a circular shape, resulting in smoother stress flow and more effective rock arching.

The preliminary finite-element modeling showed that shaft behavior was largely controlled by anisotropy, and better

correlation with measured results may be obtained with large three-dimensional, anisotropic analysis. By using a rock classification scheme, such as the "Q" system, improved correlation may also be possible between measured and theoretical results, particularly around the circular opening where the effect of rock discontinuities and elastic instabilities is reduced.

Based on the measured field data and evaluation with a preliminary finite-element analysis, the following conclusions can be drawn:

1. The circular shaft shape is least sensitive to in situ fixed conditions, particularly rock mass anisotropy.

2. A more competent, "tighter" shaft wall is produced around the circular shape following the excavation process, as indicated by the subdued nature of the rock oscillations following each blast.

3. The rectangular shape is likely to respond to in situ conditions with a variety of behavioral modes such as beam bending, buckling, and bedding plane separation.

4. Regardless of shaft shape and in situ stress field, shaft wall displacement is significantly affected by rock mass anisotropy and geologic discontinuities.

REFERENCES

1. Barton, N., F. Loset, R. Lien, and J. Lunde. Application of Q-System in Design Decisions Concerning Dimensions and Appropriate Support for Underground Installations. Subsurface Space. Pergamon, 1980, 120 pp.
2. Bathe, K. J. ADINA - A Finite-Element Program for Automatic Dynamic Incremental Nonlinear Analysis. MIT Rep. 82448-1, 1978, 200 pp.
3. Beus, M. J. Structural Design for Deep Mine Shafts--Results of Field Experiments To Determine Design Criteria. M.S. Thesis, Univ. ID, 1979, 114 pp.
4. Beus, M. J., and S. S. M. Chan. Shaft Design in the Coeur d'Alene Mining District, Idaho--Results of In Situ Stress and Physical Property Measurements. BuMines RI 8435, 1980, 39 pp.
5. Beus, M. J., E. L. Phillips, and G. G. Waddell. Instrument To Measure the Initial Deformation of Rock Around Underground Openings. BuMines RI 8275, 1978, 40 pp.
6. Chan, S. S. M., and M. J. Beus. Ground Stress Determination in the Coeur d'Alene District Using the CSIR Technique. Paper in Proceedings, Pacific Northwest Metals and Minerals Conference. AIME, Coeur d'Alene, ID, 1976, pp. 1-16.
7. _____. Interpretation of In Situ Deformational Behavior of a Rectangular Test Shaft Using Finite-Element Method. Paper in Field Measurements in Rock Mechanics, ed. by K. Kovari (Proc. Int. Symp. on Field Measurement in Rock Mechanics). A. S. Balkema, Rotterdam, v. 2, 1977, pp. 889-903.

8. Ewing, R. D., and E. M. Raney. User's Guide for a Computer Program for Analytical Modeling of Rock Structure Interaction (BuMines contract H0262020). 1976, 95 pp.; NTIS AD 761650.
9. Hobbs, S. W., A. B. Griggs, R. E. Wallace, and A. B. Campbell. Geology of the Coeur d'Alene District, Shoshone County, Idaho. U.S. Geol. Surv. Prof. Paper 478, 1965, 139 pp.
10. Hustrulid, W. Development of a Borehole Device To Determine the Modulus of Rigidity of Coal Measure Rocks (contract H0101705, CO Sch. Mines). BuMines OFR 12-72, 1971, 119 pp.; NTIS PB 209 548/AS.
11. Karwoski, W. J. Deep Shaft Design Parameters. Paper in Proceedings, Pacific Northwest Metals and Minerals Conference. AIME, Coeur d'Alene, ID, 1973, pp. 1-30.
12. Karwoski, W. J., and D. E. Van Dillon. Applications of Bureau of Mines Three-Dimensional Finite-Element Computer Code to Large Mine Structural Problems. Paper in Proceedings, 19th U.S. Symposium on Rock Mechanics. Univ. NV, Stateline, NV, 1978, v. 2, pp. 114-120.
13. Leeman, E. R. The "Doorstopper" and Triaxial Rock Stress Measuring Instrument Developed by the CSIR. J. S. Afr. Inst. Min. and Metall., v. 69, 1969, pp. 305-339.
14. _____. The Measurement of Stress in Rock. J. S. Afr. Inst. Min. and Metall., v. 65, 1967, pp. 45-144, 254-284.
15. McVey, J. R., and T. O. Meyer. An Automatic Data Acquisition System for Underground Measurements. BuMines RI 7734, 1973, 10 pp.
16. Patricio, J. G., and M. J. Beus. Determination of In Situ Modulus of Deformation in Hard Rock Mines of the Coeur d'Alene District, Idaho. Paper in Proceedings, 17th U.S. Symposium on Rock Mechanics. Univ. UT, Salt Lake City, UT, 1976, pp. 4B9-1 to 4B9-7.
17. Ranken, R. E., and J. Ghaboussi. Tunnel Design Considerations; Analysis of Stresses and Deformations Around Advancing Tunnels. Grant DOT FR30022, 1975, 200 pp.; available through NTIS.
18. Waddell, G. G., T. J. Crocker, and E. H. Skinner. Technique of Measuring Initial Deformation Around an Opening Analysis of Two Raise-Bore Tests. BuMines RI 7505, 1971, 60 pp.
19. Waddell, G. G., and E. L. Phillips. Stress Relaxation Gage. U.S. Pat. 3,600,938, Aug. 24, 1971.

APPENDIX.--BLASTING HISTORY, DISPLACEMENT TRACES, AND DISPLACEMENT RECORDS

TABLE A-1. - Blasting history of circular and rectangular test shafts

No.	Blast		Time elapsed, ¹ h	Advance per blast, ft		Total depth, ft	
	Date	Time		Approx ²	Actual	Approx ²	Actual
CIRCULAR SHAFT							
1.....	4/ 5/76	12:00 p.m.	-	1	1.5	1	1.5
2.....	4/ 5/76	3:30 p.m.	0	2	1.5	3	3
3.....	4/ 9/76	2:30 p.m.	95	3	3.5	6	6.5
4.....	4/12/76	12:45 p.m.	165	3	3	9	9.5
5.....	4/13/76	12:45 p.m.	189	3	3.5	12	13
6.....	4/19/76	2:00 p.m.	334	4	4	16	17
7.....	4/21/76	11:30 p.m.	380	4	3	20	20
8.....	4/22/76	11:30 a.m.	404	4	4	24	24
RECTANGULAR SHAFT							
1.....	6/ 4/76	10:36 a.m.	0	2	2	2	2
2.....	6/ 4/76	1:45 p.m.	3	3	3.5	5	5.5
3.....	6/ 8/76	11:00 a.m.	97	2	3.5	7	9
4.....	6/11/76	10:54 a.m.	169	4	3	11	12
5.....	6/21/76	12:45 p.m.	411	3	2.7	14	14.7
6.....	6/23/76	12:15 p.m.	458	5	6	19	³ 20.7
7.....	6/25/76	11:00 a.m.	506	5	(⁴)	26	(⁴)

¹Time elapsed since first blast following installation of the instruments.²An approximate depth facilitates reduction of data for finite-element analysis.³TSR4 anchor exposed on this blast.⁴The final depth is only approximate as the muck was not removed after the last blast.

TABLE A-2. - Circular test shaft, displacement record

Blast No.	Total depth, ft	Time elapsed, ¹ h	TSR4		TSR5		TSR6	
			MD, in	TD, in	MD, in	TD, in	MD, in	TD, in
¹ 1.....	1.5	-	-	-	-	-	-	-
2.....	3	0	0.035	0.035	-0.018	-0.018	-0.008	-0.008
3.....	6.5	95	-.009	.026	.002	-.016	.013	.005
4.....	9.5	165	.009	.035	.013	-.003	-.012	-.007
5.....	13	189	-.002	.033	.007	.004	.031	.024
6.....	17	334	-.008	.025	-.004	-.000	.006	.03
7.....	20	380	.000	.025	.002	.002	.0005	.03
8.....	24	404	.005	.03	.002	.004	.034	.064

MD Measured displacement (inches measured per blast).

TD Total displacement (inches accumulated).

¹The initial blast round defined the shaft perimeter; no data were recorded.

NOTE.--Negative sign indicates dilation of the shaft wall.

TABLE A-3. - Rectangular test shaft, displacement record

Blast No.	Total depth, ft	Time elapsed, ¹ h	TSR5		TSR8		TSR4	
			MD, in	TD, in	MD, in	TD, in	MD, in	TD, in
¹ 1.....	2	0	-	-	-	-	-	-
2.....	5.5	3	0.0075	0.0075	0.06	0.06	-0.069	-0.069
3.....	9	97	-.021	-.0135	.00	.06	.057	-.012
4.....	12	169	.024	.0105	.0285	.0885	.069	.057
5.....	14.7	411	-.0054	.0051	-.0075	.081	-.004	.053
6.....	20.7	458	-.003	.0021	-.0045	.0765	-.022	.031
7.....	26	506	.0015	.0036	-.017	.0595	-.003	.028

MD Measured displacement (inches measured per blast).

TD Total displacement (inches accumulated).

¹The initial blast round defined the shaft perimeter; no data were recorded.

NOTE.--Negative sign indicates dilation of the shaft wall.

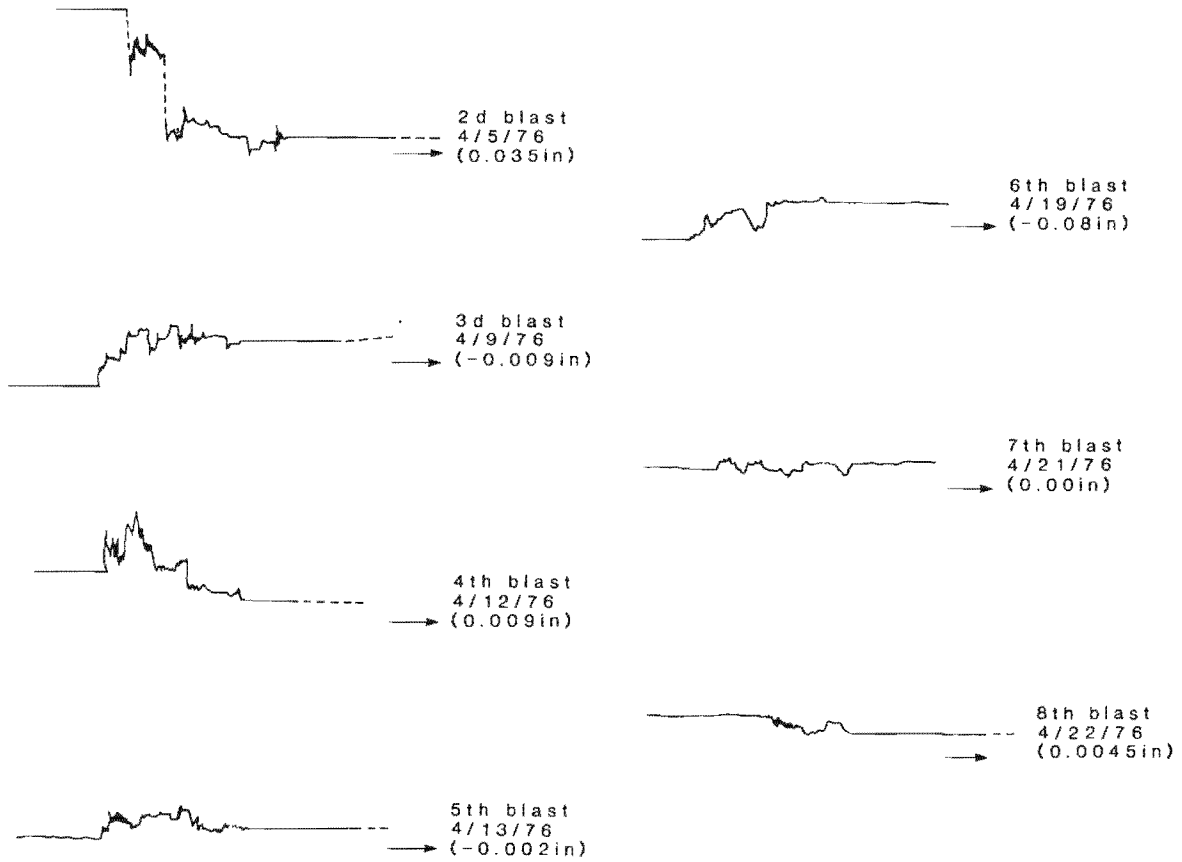


FIGURE A-1. - Displacement trace for TSR4 around circular shaft.

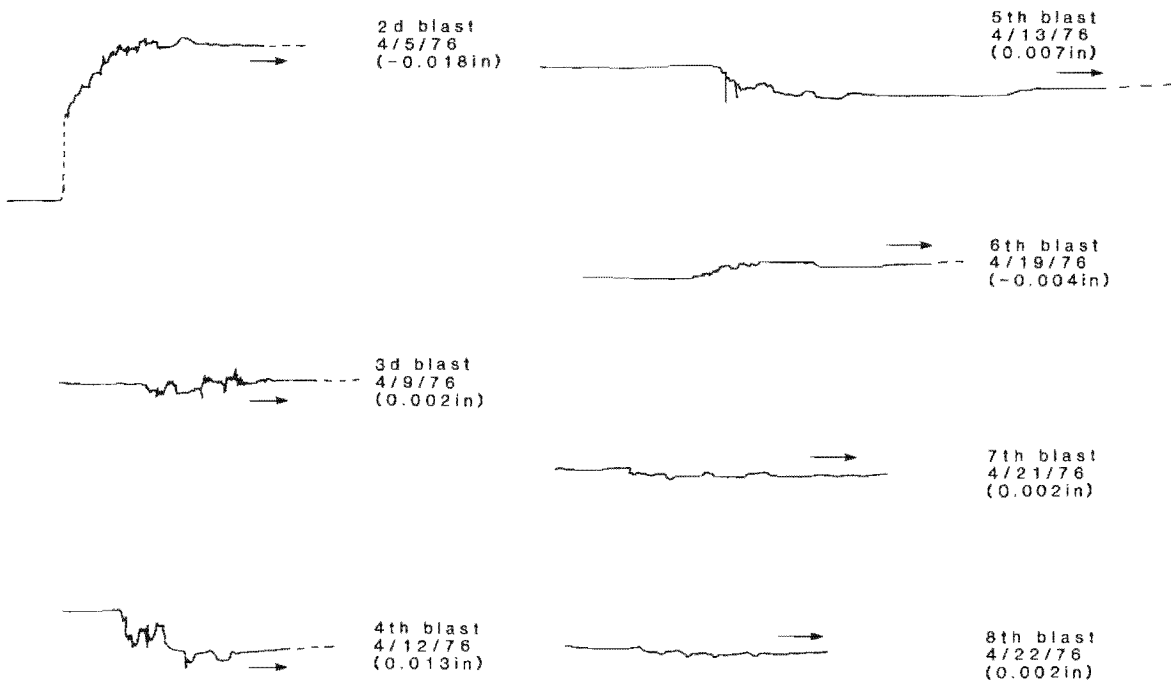


FIGURE A-2. - Displacement trace for TSR5 around circular shaft.

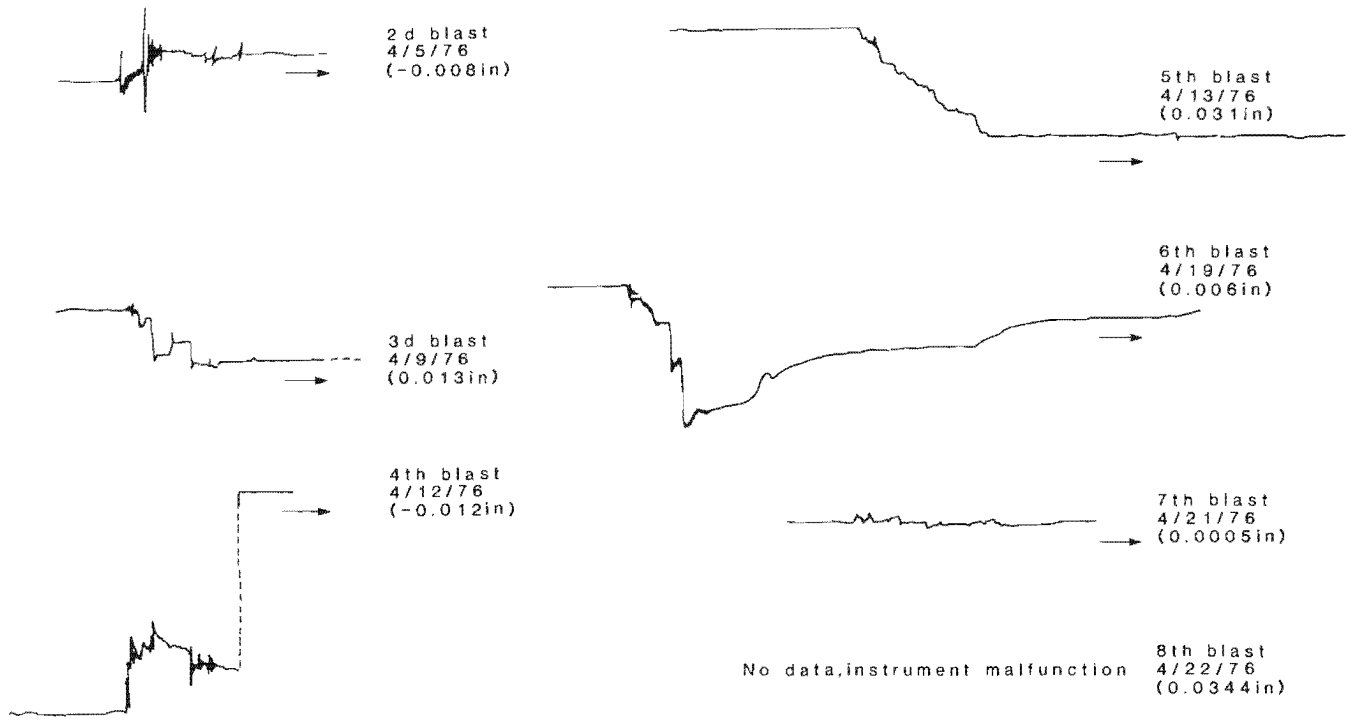


FIGURE A-3. - Displacement trace for TSR6 around circular shaft.

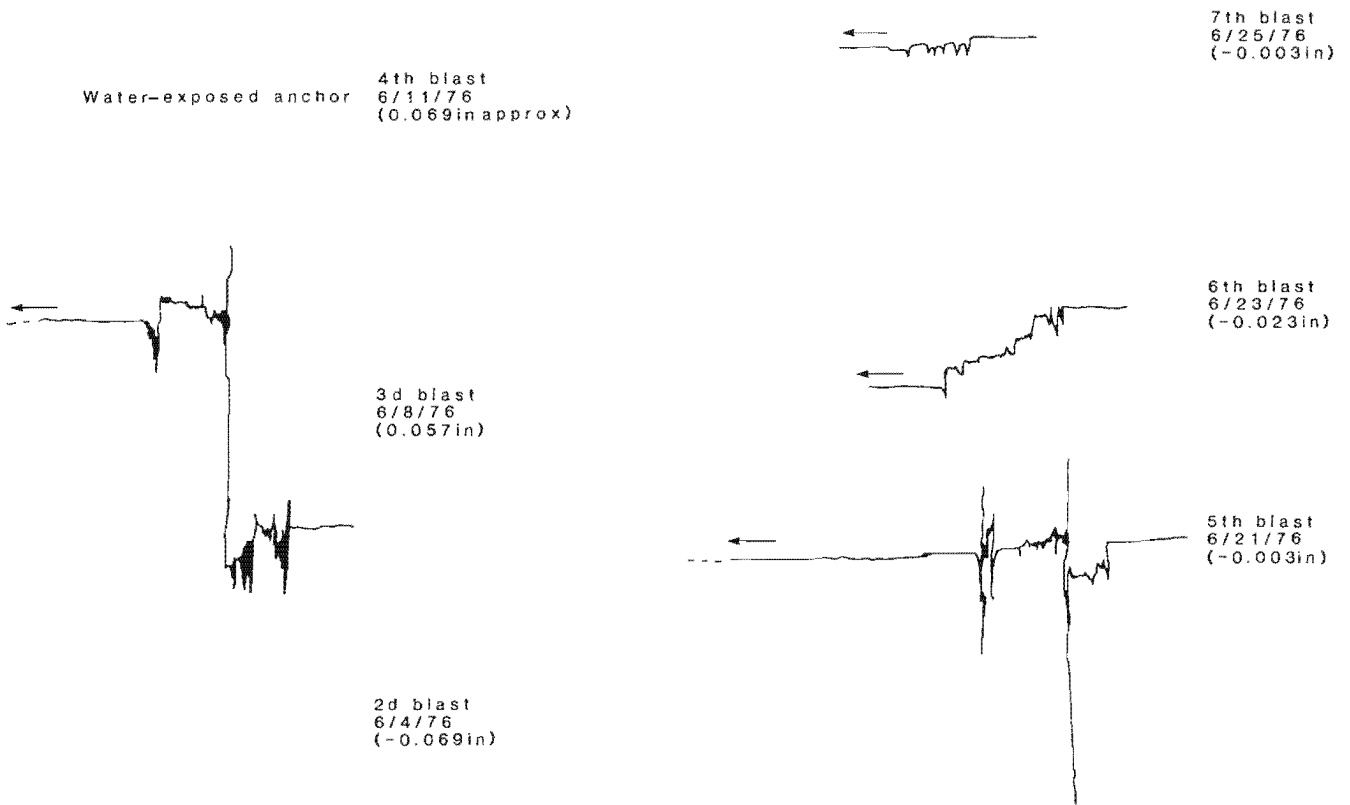


FIGURE A-4. - Displacement trace for TSR4 around rectangular shaft.

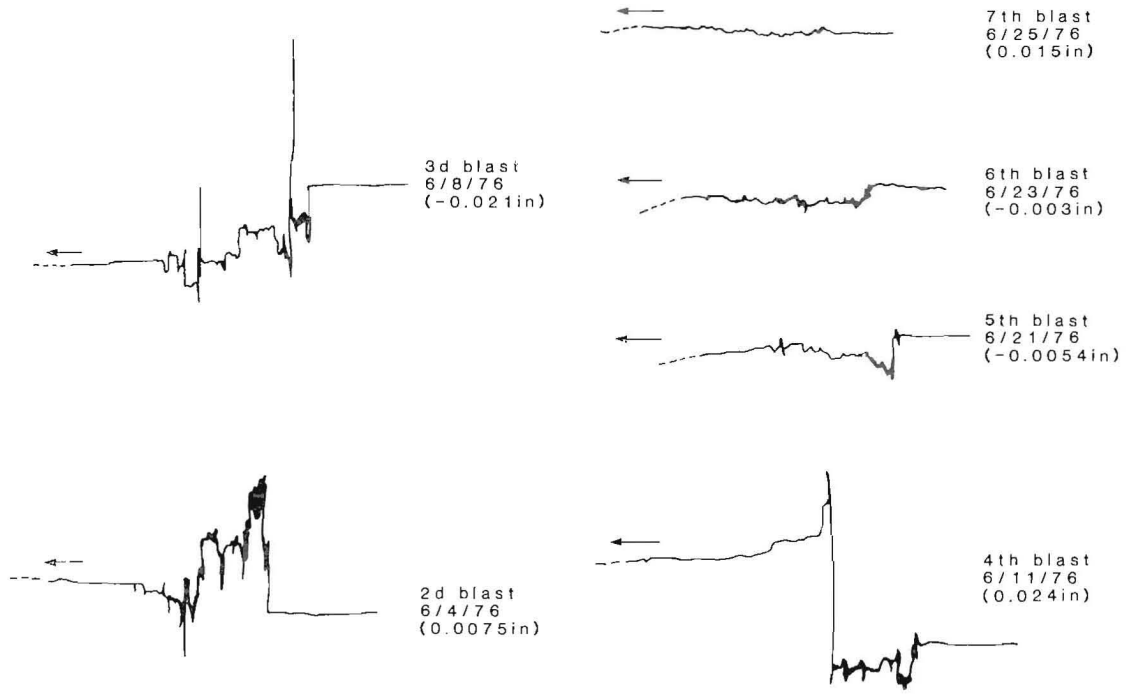


FIGURE A-5. - Displacement trace for TSR5 around rectangular shaft.

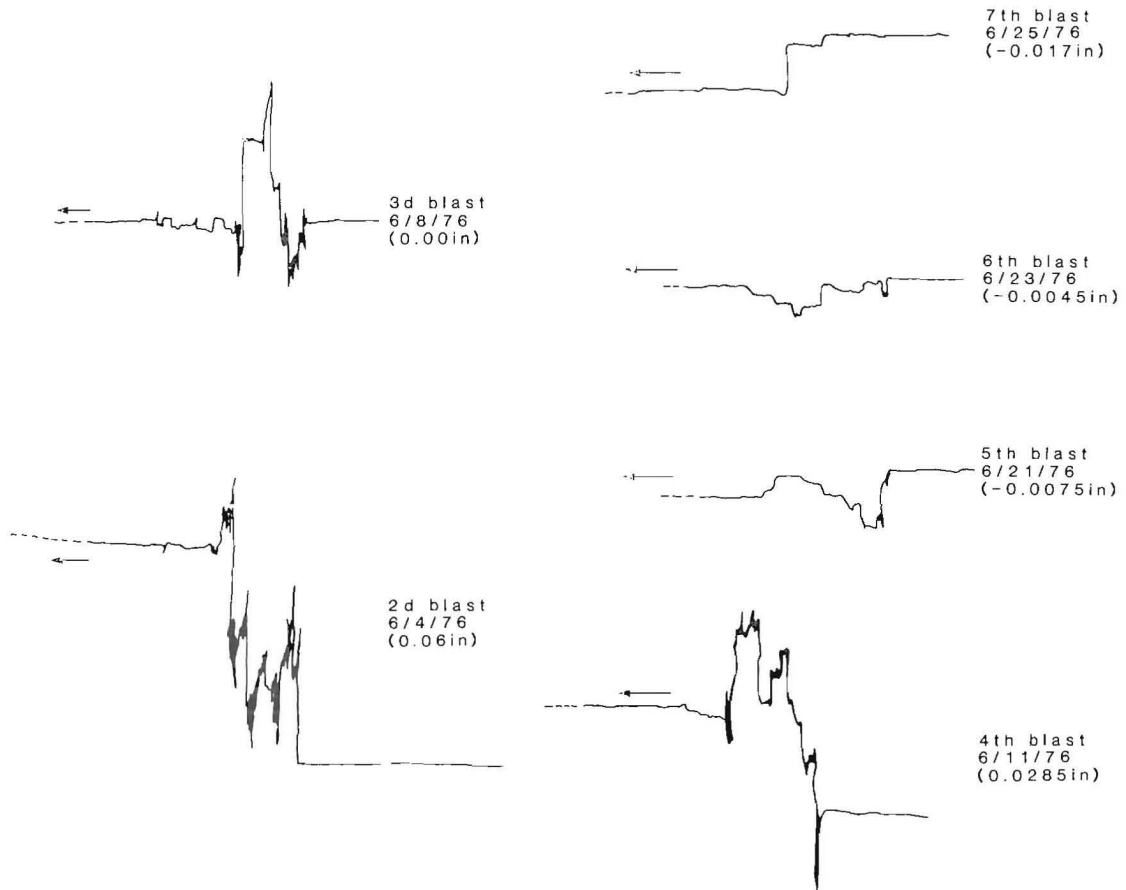


FIGURE A-6. - Displacement trace for TSR8 around rectangular shaft.